Faraday Discussions

Accepted Manuscript

This manuscript will be presented and discussed at a forthcoming Faraday Discussion meeting. All delegates can contribute to the discussion which will be included in the final volume.

Register now to attend! Full details of all upcoming meetings: http://rsc.li/fd-upcoming-meetings

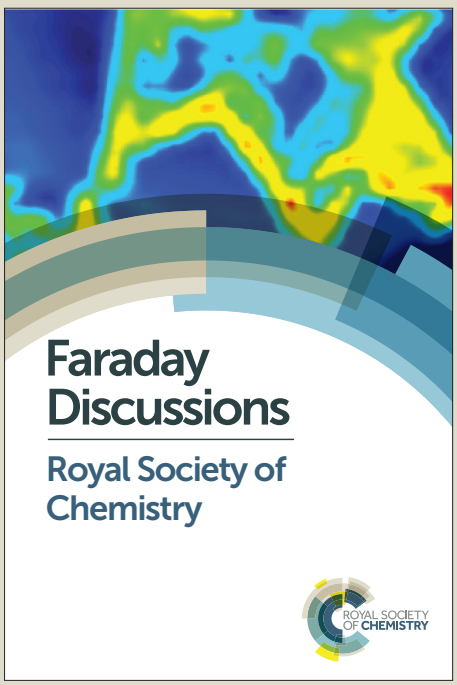

This is an *Accepted Manuscript*, which has been through the Royal Society of Chemistry peer review process and has been accepted for publication.

Accepted Manuscripts are published online shortly after acceptance, before technical editing, formatting and proof reading. Using this free service, authors can make their results available to the community, in citable form, before we publish the edited article. We will replace this *Accepted Manuscript* with the edited and formatted *Advance Article* as soon as it is available.

You can find more information about *Accepted Manuscripts* in the Information for Authors.

Please note that technical editing may introduce minor changes to the text and/or graphics, which may alter content. The journal's standard Terms & Conditions and the Ethical guidelines still apply. In no event shall the Royal Society of Chemistry be held responsible for any errors or omissions in this *Accepted Manuscript* or any consequences arising from the use of any information it contains.

ROYAL SOCIETY OF CHEMISTRY

www.rsc.org/faraday_d

Journal Name

ARTICLE

Sequential nested assembly at the liquid/solid interface

Baharan Karamzadeh,[a] Thomas Eaton,[b] David Muñoz Torres,[b] Izabela Cebula,†[a] Marcel Mayor*[b,c,d] and Manfred Buck*[a]

Received 00th January 20xx,
Accepted 00th January 20xx

DOI: 10.1039/x0xx00000x

www.rsc.org/

Studying the stepwise assembly of a four component hybrid structure on Au(111)/mica, the pores of a hydrogen bonded bimolecular network of 3,4:9,10-perylenetetracarboxylic diimide (PTCDI) and 1,3,5-triazine-2,4,6-triamine (melamine) were partitioned by three and four-armed molecules based on oligo([biphenyl]-4-ylethynyl)benzene, followed by the templated adsorption of either C_{60} fullerene or adamantane thiol molecules. The characterisation by ambient scanning tunneling microscopy (STM) reveals that the pore modifiers exhibit a dynamics which pronouncedly depends on the molecular structure. The three-armed molecule 1,3,5-tris([1,1'-biphenyl]-4-ylethynyl)benzene (3BPEB) switches between two symmetry equivalent configurations on a time scale fast compared to the temporal resolution of the STM. Derivatisation of 3BPEB by hydroxyl groups substantially reduces the switching rate. For the four-armed molecule configurational changes are observed only occasionally. The observation of isolated fullerenes and small clusters of adamantane thiol molecules, which are arranged in a characteristic fashion, reveals the templating effect of the trimolecular supramolecular network. However, the fraction of compartments filled by guest molecules is significantly below one for both the thermodynamically controlled adsorption of C_{60} and the kinetically controlled adsorption of the thiol with the latter causing a partial removal of the pore modifier. On the one hand, demonstrating the feasibility of templating by nested assembly, the experiments, on the other hand, pinpoint the requirement for the energy landscape to be tolerant to variations in the assembly process.

Introduction

Supramolecular assembly at interfaces has been widely studied both in ultrahigh vacuum (UHV) and at the solid-liquid interface. Providing convenient access to the sub-5 nm length scale with atomic precision,[1-25] 2D networks are of particular interest as they enable ultraprecise templating by exploiting interactions of guest species with the network structure and/or defining adsorption sites through the confinement of guest entities to network pores.[5, 18, 26-40]
Strategies for the generation of structures comprise either the simultaneous assembly of multicomponent systems to complex patterns[41] or a sequential step by step procedure.[28, 34] The former is accomplished under thermodynamically controlled conditions involving well designed interactions and geometries of the individual components. The latter can be performed either under thermodynamic or kinetic control, thus offering more degrees of freedom. Notably, guest species which are thermodynamically more stable than the network and, thus, ultimately displace it, can be templated.[42] Furthermore, very different types of steps can be combined[43] and the network can serve as a temporary sacrificial mask.[44] However, apart from the underpotential deposition of Cu following the pore filling of a network by a thiol[43] and the generation of a binary SAM by replacement of the network,[44] sequential assembly has not been going beyond the two steps of network formation and adsorption of a guest species. The supramolecular template defining the arrangement of the guest in this case, any changes will require the adaptation of the network by varying the pore size and/or geometry[28] or functionalising the pores by derivatisation of the network components.[45, 46]
A complementary, yet unexplored strategy for the stepwise generation of surface based nanostructures is nested self-assembly. As illustrated in Fig. 1, the structure of a porous molecular network which defines the base frame, is modified prior to the adsorption of guest species. While this strategy offers an additional level of structural control, it will require precise matching of components as regards both geometries and interaction energies. Important aspects in this context are the affordable tolerances in the dimensions of the pore modifier and the influence of a highly confined space on the assembly process with the latter being particularly important

[a] EaStCHEM of School Chemistry, University of St Andrews, North Haugh, St Andrews,United Kingdom. E-mail: mb45@st-andrews.ac.uk.
[b] Department of Chemistry, University of Basel, St. Johannsring 19, CH 4056 Basel, Switzerland. E-mail: marcel.mayor@unibas.ch
[c] Institute of Nanotechnology, Karlsruhe Institute of Technology (KIT), P.O.Box 3640, D-76021 Karlsruhe, Germany.
[d] Lehn Institute of Functional Materials (LIFM), Sun Yat-Sen University (SYSU), Guangzhou, P. R. China.
† Present address: Department of Chemical and Process Engineering, University of Strathclyde, James Weir Building, 75 Montrose Street, Glasgow G1 1XJ, United Kingdom.
Electronic Supplementary Information (ESI) available: Details of chemical synthesis of **4BPEB-2OH** and additional STM images. See DOI: 10.1039/x0xx00000x. The research data supporting this publication can be accessed at http://dx.doi.org/10.17630/3a666470-8a12-466c-8baf-d0335b4ad97a.

for the solid/liquid interface where the adsorption of species involves an exchange of solvent molecules. The studies reported here build on our previous work where, in experiments examining a series of threefold symmetric star-shaped molecules differing in size, tris([biphenyl]-4-ylethynyl)benzene (**3BPEB-H**, see Fig. 1) was identified as the one fitting the pores of a hydrogen bonded honeycomb network.[47] Having observed that **3BPEB-H** exhibits a dynamic behaviour one focus of the present study is on the underlying mechanism and factors affecting it. This includes modification of the molecules by both chemical functionalisation and addition of a fourth arm (see Fig. 1). It is noted that there are two equivalent threefold degenerate configurations for the threefold symmetric star molecules (ignoring the asymmetry introduced by the OH groups) whereas the degeneracy is lifted for **4BPEB-2OH**, thus resulting in six equivalent positions. The other focus is the templating of the star/network structure using C_{60} fullerene and adamantane thiol. $C_{60,}$ a commonly used guest molecules in surface based self-assembly,[6, 27, 28, 30-35, 39, 46, 48-51] and the much less studied thiols[42, 44, 45, 52] have been chosen as representatives for assembly under thermodynamic and kinetic control.

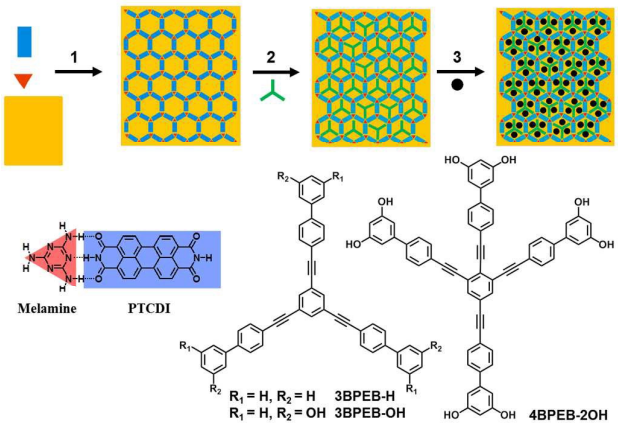

Fig. 1 Top: Scheme of sequential molecular assembly comprising formation of a bimolecular honeycomb network of PTCDI and melamine (1), compartmentation of the network pores (2), and adsorption of guest molecules into the subpores (3). Bottom: Structures of the molecules used.

Results and Discussion

Synthesis

The syntheses of the star-shaped guest molecules are based on Pd catalysed coupling chemistry.[53] While the syntheses of the two three-armed stars **3BPEB-H** and **3BPEB-OH** were already reported elsewhere,[47] the assembly of the four-rayed star **4BPEB-2OH** is sketched in Scheme 1. As central unit a fourfold 1,2,3,5-ethynyl-substituted benzene was required, which was obtained from the commercially available 2,4,6-tribromoaniline **6**, which was converted to the 1,3,5-tribromo-2-iodobenzene **7** using a variation of the *Sandmeyer* reaction.[54]

Subsequent treatment with a twelvefold excess of 2-methylbut-3-yn-2-ol under *Sonogashira* coupling conditions gave the fourfold ethynyl substituted benzene **8**, which provided the central building block **9** after deprotection. Treatment of the 1,2,3,5-tetraethynylbenzene **9** with four equivalents of the iodo-biphenyl derivate **5** again under *Sonogashira* conditions provided the four-armed star **4PBEP-2OH** as brown solid in 45% isolated yield after column chromatography. The assembly of the 4'-iodo-[1,1'-biphenyl]-3,5-diol **5** is displayed in scheme 1 and is based on *Suzuki* coupling combined with suitable masking strategies.

The four-armed star **4PBEP-2OH** was characterized by ^{1}H- and ^{13}C-NMR spectroscopy and by mass spectrometry. The identity of the structure was further corroborated by its appearance in the STM experiments reported in this paper. Synthetic protocols and analytical data of all new chemical structures are provided in ESI.

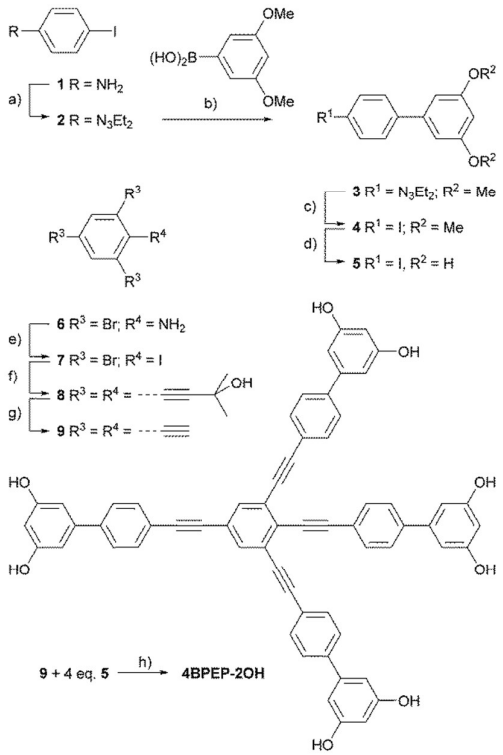

Scheme 1 Synthesis of the four-armed star structure **4BPEB-2OH**. Reagents and conditions: a) conc. HCl, aq. $NaNO_2$, Et_2NH, K_2CO_3, 0°C to RT., 53%; b) $Pd(PPh_3)_2Cl_2$, K_2CO_3, $C_6H_5CH_3$, EtOH, MicroWave, 120°C, 45 min., 56%; c) MeI, 130°C, 90%; d) BBr_3, CH_2Cl_2, -78°C, 79%; e) 1.) $pTsOH{\cdot}H_2O$, $NaNO_2$, KI, CH_3CN, H_2O, 15˚C, 10 min.; 2.) 20˚C, 2h, 68%; f) 2-methyl-3-butyn-2-ol, $Pd(PPh_3)_2Cl_2$, CuI, DMF, Et_2NH, 80˚C, 24h, 49%; g) NaH, $C_6H_5CH_3$, 120˚C, 3h, 49%; h) $Pd(PPh_3)_4$, CuI, THF, iPr_2NH, 45˚C, 16h, 45%.

Surface Studies

I. Compartmentation of network pores

Exposure of the PTCDI-melamine network to **3BPEB-H** yields images like those depicted in Fig. 2. While the network is well resolved with both the melamine and PTCDI components clearly seen, the characteristic star shape of the pore modifier

appears only occasionally like in the marked pore in the upper half of Fig. 2a. In such cases where even the individual benzene rings of the **3BPEB-H** molecule are resolved, the occurrence of the star shape is typically accompanied by at least one additional protrusion like the one marked by the arrow in Fig. 2a which indicates the presence of additional trapped species.

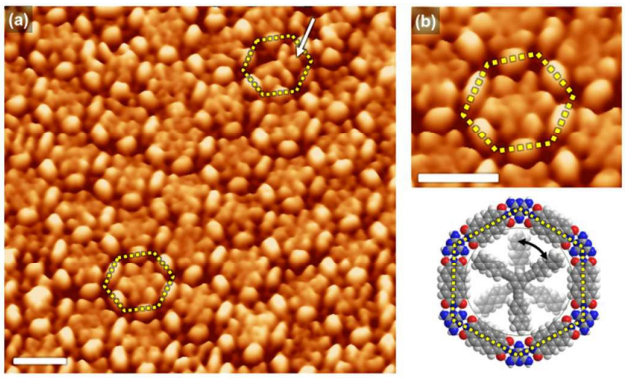

Fig. 2 High resolution STM images in 3D representation of **3BPEB-H** adsorbed in the pores of a supramolecular network composed of PTCDI and melamine. (a) Larger scale image with two pores highlighted, one showing the star molecule (top), the other one a sixfold pattern. Arrow marks an additional species trapped in the star modified network pore. (b) Magnified image of the pore exhibiting a sixfold pattern with structural model indicating a switch between the two equivalent positions of the star molecule. Scale bars: 3 nm.

However, in more than 90% of the pores other patterns are seen with the highly symmetric sixfold pattern shown in Fig. 2b being the dominating one. An obvious interpretation of the sixfold pattern is, as illustrated by the molecular model of Fig. 2b, a fast switching of the molecule between the two equivalent positions, so a superposition of both configurations is seen. To verify this, experiments were performed with **3BPEB-OH**. The three additional OH groups compared to **3BPEB-H** should increase the interaction of the star molecule with the network and/or the substrate and, thus, affect the switching rate of the molecule, similar to a monocomponent system[55, 56] which demonstrated a packing dependent influence of sterical factors and intermolecular interaction on molecular rotation. This is fully confirmed as evidenced by the STM image shown in Fig. 3a-i. The star shape of the molecule is now clearly visible in most of the pores whereas the sixfold pattern, highlighted by the circle in Fig. 3a-i, is observed at a level of less than 10%. In some of the pores which display the threefold geometry, additional species are trapped. As illustrated in Fig. 3a-ii these can be sufficiently big like a residual PTCDI to cause a deformation of the star.[47] However, there are also features visible such as the cross-like geometry shown in Fig. 3a-iii which do not correlate with the structure of the star molecule in an obvious way. While the clear appearance of the shape of the molecule in Fig. 3a-i suggests that the molecules are now locked into place, a closer look at the patterns reveals that also **3BPEB-OH** exhibits a dynamic behaviour. As documented in Fig. 3b which shows a series of images of the same pores recorded over a period of time of about 6 min, significant changes occur. Except for pore 2 where the sixfold pattern is essentially preserved, the appearance of the other pores change markedly, yet in pronouncedly different ways. In pores 1 and 5 the star shape appears intermittently (1-iii, 5-ii) among a sixfold pattern. A different case is seen in pore 3 where the star shape is seen throughout the sequence but a switch in orientation occurs between images iii and iv as highlighted by the magnified images of pore 3 seen in Fig. 3c. Another noteworthy feature of this pore is that in some images (iii and iv) the biphenyl moiety appears to be resolved whereas in most other cases

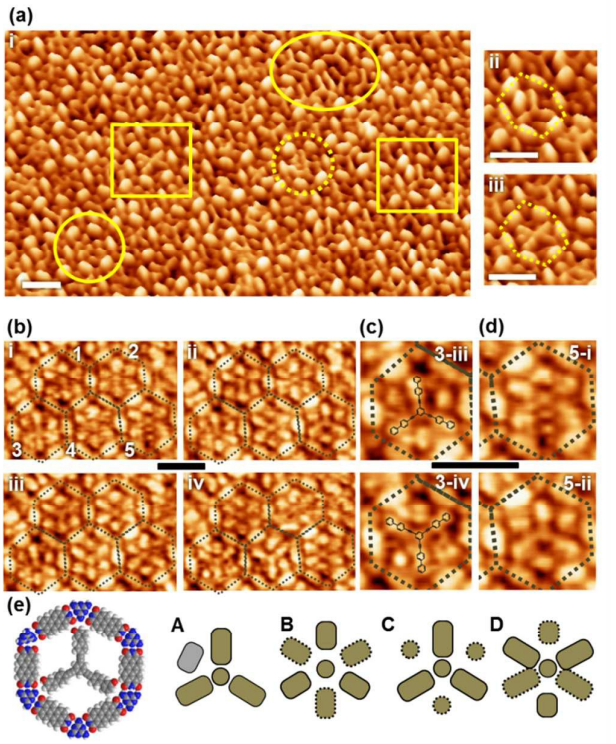

Fig. 3 STM images of **3BPEB-OH** adsorbed in the pores of a PTCDI-melamine network. a) 3D representation of the structure with rectangles framing the pores shown on the right on an enlarged scale. Pore encircled by solid line highlights a sixfold pattern, dotted circle marks am irregular patterns and the ellipse marks an area of a network defect. (b) Sequence of four STM images of the same area of the **3BPEB-OH**/network structure recorded over a period of time of about 6 min. The network is indicated by the dotted lines. (c,d) Close-ups of pores 3 and 5 for the images as indicated. For pore 3 the images are overlaid with the structure of **3BPEB-OH**. (e) Structural model of **3BPEB-OH** in the network pore and schematic representations of pore patterns (A-D) observed for **3PBEB-H** and **3PBEB-OH**. Scale bars: 3 nm.

only more or less elongated protrusions are seen. Pore 4 also exhibits an interesting time behaviour as it evolves from a sixfold symmetry in image i to a threefold symmetry in image iv with a mirror symmetric appearance in image ii, caused by a slightly elongated shape of four of the protrusions which resembles the cross-like geometry depicted in Fig. 3a-iii. Such a temporary cross-like feature is also seen for pore 5 as seen from the comparison of the enlarged images of the pore in Fig. 3d. From this it can be concluded that the cross-type shape arises from the dynamics and imaging of the molecule and not

from a different molecular species. Noting that some of the pores exhibit irregular features (for an example see dotted circle in Fig. 3a-i), Fig. 3e summarizes the different regular patterns observed for **3BPEB-H** and **3BPEB-OH** together with a structural model

Of the various patterns A and B are straightforward to explain with A, as discussed previously,[47] showing a star molecule locked into place by an additional species and B, as mentioned above, resulting from the superposition of two equivalent configurations. To produce pattern B which is prevalent in **3PBEB-H**, the switching rate has to be fast compared to the temporal resolution of the STM. While our ambient experiments do not allow us to determine the switching rate an idea of its value may be obtained by comparing our images with those from UHV studies where switching rates have been quantified and Arrhenius parameters be determined for a porphyrine derivative on top of a supramolecular network pore,[57] dibutylsulfide on Au,[58] and a sexiphenyl-trimer inside a hexagonal network pore.[59] The comparison is based on the observation that at sufficiently high temperatures the images appear as a smooth superposition of the different configurations whereas at lower temperatures images become frizzy or even the individual configurations are seen. The smooth sixfold pattern seen for 3BPEB-H would be compatible with a switching rate in the range of $10^4 - 10\ s^{-1}$ by taking Fig. 2 of ref. 58 and Fig. 3 of ref. 59 as reference.

The discrete sixfold pattern suggests that the two equivalent configurations, where the arms of the molecule point to the vertices of the pore, are long lived compared to any intermediate configurations. Otherwise one would expect a different pattern such as a toroidal structure as seen for hexa-*tert*-butyl decacyclene[60] or coronene[61] as resulting from a continuous and random rotational motion. This raises the question of how the transition between the two states occurs.

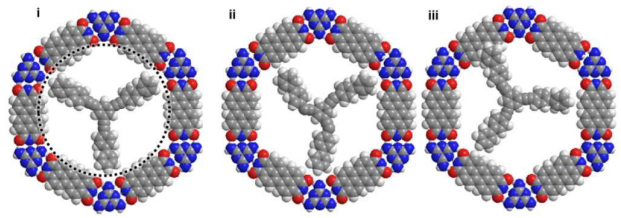

Fig. 4 Models of **3BPEB-H** in one of the two stable configurations (i), a transition state with the molecule confined to two dimensions (ii), and a transition state allowing part of the molecule to detach from the surface (iii). The size of the undistorted **3BPEB-H** star in (i) is based on crystallographic data[62] and drawn at the scale of the network pore. The dotted circle in (i) frames the area assuming a rigid geometry of the star molecule.

Looking at the models shown in Fig. 4, a purely rotational step is not possible for sterical reasons as indicated by the dotted circle in structure i if one assumes that the molecule is rigid and the molecule is confined to two dimensions, i.e., all parts of the molecule are always in contact with the surface. Even if one takes into account that the ethynyl bonds exhibit considerable flexibility,[63-66] they would have to be deformed to an extent (more than 60°) which seems unreasonable (structure ii). Including the third dimension by allowing the molecule to partially detach, the deformation of the molecule during a rotational step can be limited to its normal flexibility by one arm passing above a PTCDI molecule (structure iii). The latter scenario is corroborated by studies on the dynamical behaviour of sexiphenyldicarbonitrile molecules in a honeycomb network where a hopping between pores was reported to already occur well below room temperature.[67] This system is also interesting as these molecules form a trimer structure with a threefold symmetry, thus yielding a caged structure very similar in geometry to ours. In a detailed experimental study[59] they observe rotations of the trimeric entity already at temperatures well below 100 K. Molecular dynamics simulations reveal the details of the rotational mechanism.[67] In this case it can be restricted to two dimensions since, in contrast to our covalent star structure, the trimer structure allows for a dynamical adaptation to the geometry of the network during the transition between two states. This is afforded by weak supramolecular interactions which provides more degrees of freedom such as frustrated rotations of the individual components and changes in the phenyl hydrogen/CN bonds.

As far as the patterns **C** and **D** (Fig. 3e) are concerned they are less straightforward to explain and at this point we can only speculate on their origin. Pattern **C** still exhibits a threefold symmetry which suggests that it derives from a rotational motion of the star molecule. It can be viewed as a weighted six-fold pattern where the degeneracy of the two configurations is lifted, so the average dwell time of the star molecule is now different for the two configurations. Possible reasons for lifting the degeneracy could be a small deformation of the pore or a contamination such as a solvent molecule trapped at a vertex of a pore. An example of such a pattern is pore 1 in Fig. 3b-iii. It is noted that small changes in geometry could also affect the tunnelling contrast and, thus, the appearance of the molecule. This could explain why in some cases the threefold symmetry seems broken like in image iv of pore 3 (Fig. 3b,c). The explanation of pattern **D** which exhibits mirror symmetry is even more speculative. Deviating from the threefold symmetry of the system an imaging effect is the most obvious explanation if opposing vertices are associated with a loss of contrast. This can arise from a dynamic effect, i.e., the arm pointing towards this direction retains some mobility due to a weaker interaction with the substrate.

Based on the proposed mechanism of rotation, the decrease in the rate of rotation for **3BPEB-OH** compared to **3BPEB-H** is associated with the increased interaction of the OH group with the network and the substrate, thus resulting in a higher activation barrier for detachment of one arm. It is noted that such a detachment should also involve a rotation around the long axis of the arm which would result in a dynamic statistical distribution of all OH groups across the 12 equivalent positions.

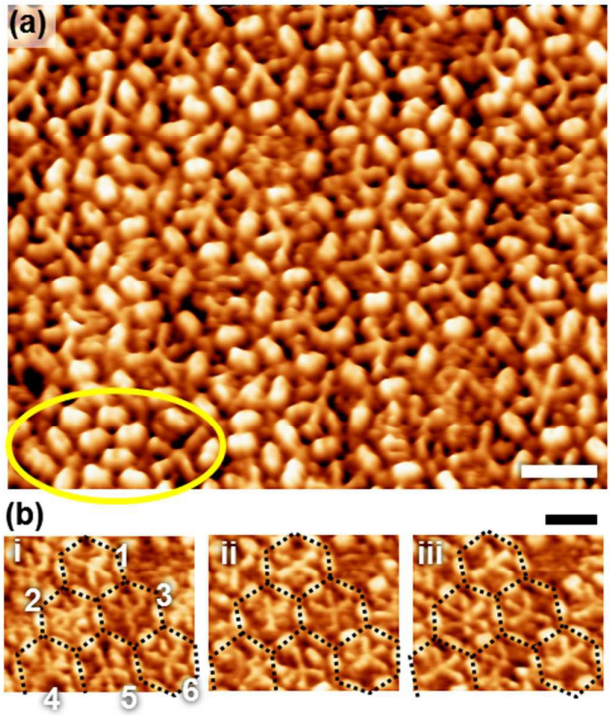

Fig. 5 STM images of **4BPEB-2OH** adsorbed in the pores of a PTCDI-melamine network. (a) Overview showing the four-armed molecule locked in the pores. Yellow ellipse marks a defect in the network. (b) Illustration of the dynamics of the molecules by a sequence of images of the same pores recorded over a period of time of 2.5 min. Scale bars: 3 nm

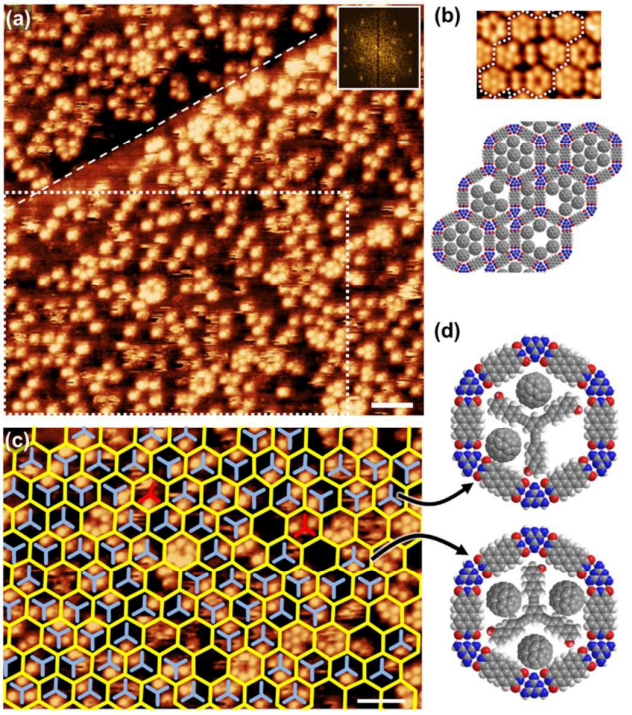

Fig. 6 STM images of C_{60} adsorbed onto a Au/mica substrate patterned by a **3BPEB-OH**/network structure. (a) Overview image with inset showing the Fourier transform. Dashed line marks a substrate step. (b) STM image (same scale as image (a)) and model of the area framed by the dashed line showing various arrangements of fullerenes in a network without star molecules. Small pores at packing faults of the network can accomodate two close-packed fullerenes. (c) Enlarged image of the section marked by the dotted rectangle in (a) with network structure and star molecules overlaid. Red stars indicate compartmentation where the **3BPEB-OH** molecules have to be deformed to fit. (d) Models of star modified pores accomodating two or three fullerenes. Scale bars: 5 nm.

Extending the experiments to **4BPEB-2OH**, the STM image presented in Fig. 5a evidences that this less symmetric molecule also adsorbs in the network pores. In the large majority of pores the shape of the molecule with its four arms is clearly resolved. In contrast to the three-armed molecules presented above no sixfold symmetric states are seen which indicates a further slow-down of the dynamics owing to the additional interactions of the extra arm and the second OH groups of **4BPEB-2OH**. However, the molecules still undergo rotation as illustrated in the sequence of images shown in Fig. 5b. Comparing images i and iii, changes in the orientation of the molecules occur in pores 1, 3, and 6. The lower symmetry of the molecules reveals (modulo 6) the number of rotational steps and the direction of rotation. The former is one and the latter has to be random as the system is in thermodynamic equilibrium. It is noted that the feature seen in image ii of pore 1 does not reflect the molecular shape but shows a cross-like geometry similar to the one observed for **3PBEB-OH**. Again, the fact that one sees the molecular structure in images i and iii points to a dynamical and/or imaging effect.

II. Adsorption of guest species

The hybrid structure composed of the PTCDI-melamine network and the **3BPEB-OH** or **4BPEB-2OH** molecules were exposed to either C_{60} fullerene or adamantane thiol. Looking first at the results for C_{60} which are compiled in Figs. 6 and 7 for **3BPEB-OH** and **4BPEB-2OH**, respectively, both systems do not produce any obvious regular arrangement of the fullerene molecules. However, the Fourier transforms shows peaks which indicates that the distribution of the C_{60} molecules is not random.

Since the network itself is not resolved when the C_{60} is present, pores without a star molecule serve as reference points as they are revealed by characteristic clusters of C_{60} involving 6-7 molecules like those shown Fig. 6b. As seen from the overlay images (Fig. 6c, Fig. 7) the position of the fullerenes fit nicely to the network/star structure, thus, revealing the templating effect of the star/network hybrid structure. The reason why the images look irregular is the lack of perfection as regards the filling of the compartments. Instead of the maximum number of fullerenes per network pore, which is three for **3BPEB-OH** and two for **4BPEB-2OH**, the majority of pores show only 1 or 2 fullerenes in the case of **3BPEB-OH** and only 1 for **4BPEB-2OH**. The low number of fullerenes in a pore already indicating the presence of the pore modifier, further evidence comes from the distance between the fullerenes. They are well separated by about 18 Å which is distinctly more than the 10 Å of paired fullerenes as seen in the small pores of Fig. 6b. It is noted that, due to the lack of

intermolecular stabilisation, imaging of the isolated C_{60} is more delicate compared to pairs or clusters of C_{60} as depicted in Fig. 5b. This is reflected in the occasional occurrence of short streaks or the imaging of a fraction of a C_{60} molecule before it is moved by the tip.

The filling of only a fraction of the compartments can be explained by sites being blocked by another species such as a trapped solvent molecule, an unknown contamination due to the handling in an ambient environment, or residual components of the PTCDI-melamine network. Importantly, this does not only mean a complete steric blocking of an adsorption site but includes any factors which influence the adsorption energy of the C_{60}. Lacking the stabilising interactions between C_{60} molecules adsorbed in larger pores,[34, 45, 46] minor changes in the environment can affect the energy landscape to the extent that adsorption of an isolated C_{60} molecule becomes unfavourable.[6] While it is also dependent on the preparation condition, it is noted in this context that templated adsorption of isolated fullerenes with high yield is rather the exception[21, 30, 35] than the rule.[27, 28, 31-33, 46, 51]

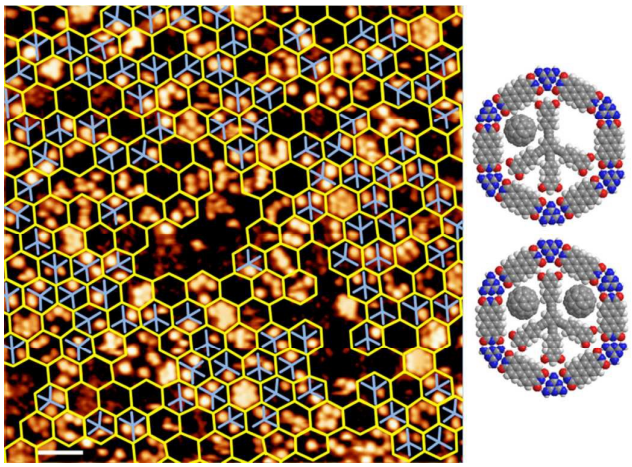

Fig. 7 STM image of C_{60} adsorbed onto a Au/mice substrate patterned by a **4BPEB-2OH**/network structure with network and pore modifier overlaid in areas where the fullerenes map the network pattern. For the original image and its Fourier transform see Fig. ESI1. On the right, models of network pores filled with **4BPEB-2OH** and one or two separated fullerenes are shown.

The adsorption of C_{60} being sensitively dependent on the energy landscape it is of interest to study guest species which have a higher driving force for adsorption. Choosing adamantane thiol which forms a rather strong S-Au bond and is sterically less demanding than C_{60}, the question arises how this fits into the energy landscape of the pore modified hybrid structure. In contrast to C_{60}, which interacts with the surface and the network/star structure relatively weakly and, thus, can be adsorbed under thermodynamically controlled conditions, adamantane thiol which has already been successfully adsorbed into the pores of an unmodified PTCDI-melamine network,[42, 44] requires kinetic control. While adamantane thiol does not displace the network,[42] it can displace the star molecules as seen in tests on uniform layers of the star molecules. Indeed, adsorption at room temperature does not produce a clear signature of the compartmentation by the 3BPEB-OH star but clusters of adamantane thiol molecules are seen which are similar to those observed for the network without the star molecules. In line with the above discussed dynamics involving a thermally induced temporal detachment of the arms, we conclude that adamantane thiol quite easily displaces the pore modifier. In an attempt to reduce the dynamics, thiol adsorption was performed at lower temperature, i.e., the melting temperature of the solvent. As seen from Fig. 8, adamantane thiol which is molecularly resolved as bright protrusions, easily adsorbs also at cryogenic temperatures. Overlaying the hexagonal network based on the original image and the Fourier filtered image which are provided in Fig. ESI2, reveals that a significant fraction of the network pores display clusters of 10-15 molecules, thus indicating removal of the star molecules even at this low temperature. However, in a number of pores the adamantane thiol is present as either an individual molecule or small aggregates of 2 to 4 molecules. A closer look reveals that specific arrangements are realised which indicate compartmentation of the hexagonal pore by the star molecules. Different cases can be identified which are marked by the green, red, and white stars. In pores with green stars the arrangement of the protrusions is in agreement with **3BPEB-OH** being present in an undistorted geometry while pores labelled by the red stars can only be described by a slightly distorted geometry. Some configurations, labelled by the white stars, require an even larger displacement with one arm detached. However, this interpretation has to be taken with a grain of salt as such cases are not very frequent, thus, raising the question of other possibilities such as the combination of some contamination and thiol molecules coincidentally resulting in a pattern suggesting the presence of the star molecule. In pores with the undistorted star geometry one to four thiol molecules are observed per compartment. Models labelled A and B in Fig. 8 provide specific examples of how the thiols can be arranged. While the maximum of four molecules per compartment packs the thiols densely and thus enforces a diamond shaped geometry, variations in the positions are seen for 1-3 molecules. It is noted that the maximum number of 12 molecules per pore, i.e., four in each compartment, have not been observed. Rather a mix involving one to four molecules is seen or even only one compartment being filled like in the case of pore A. However, the latter does not necessarily mean that the other two compartments are empty. It is conceivable that for less than 4 molecules any features are smeared out due to a fast diffusion and rearrangement of the thiols. A dynamic behaviour can also explain brighter features which either lack the distinct pattern of densely packed thiol molecules (e.g. pore D) or exhibit protrusions like the ones indicated by the circles in model B, which are too close to each other to be explained by discrete molecules. Analogous to the above discussion of the dynamics of the star molecules, the different features are interpreted to arise from different time scales involved in the dynamical behaviour of the molecules.

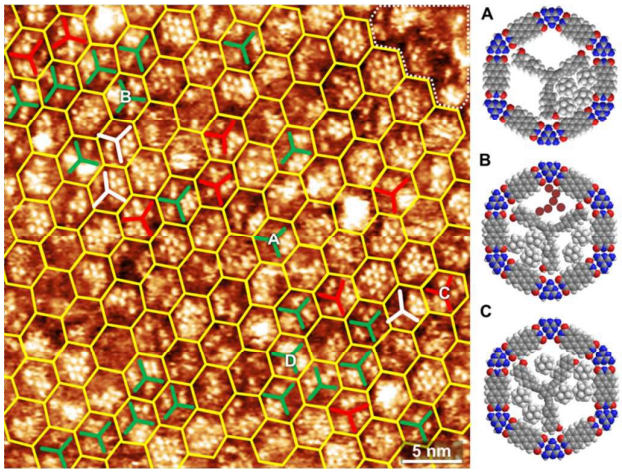

Fig. 8 Left: STM image of a **3BPEB-OH** modified PTDCI-melamine network on Au/mica after immersion in a 10 μmolar solution of adamantane thiol in ethanol at a temperature of -111°C and an immersion time of 45 s. The PTCDI-melamine network is indicated by yellow hexagons. Dotted white line in upper right corner marks an area where no network is discernible. Compartmentation by undistorted and distorted **3BPEB-OH** molecules is indicated by green and red stars, respectively. White stars indicate cells where star molecules, if present, must be dislocated. Right: Models of specific configurations with letters A-C labelling the respective pores in the STM image. For details see text.

The experiments presented above demonstrate the principle of refinement of a structure by nesting and templating under either thermodynamic (C_{60}) or kinetic control (adamantane thiol). At this point we would like to briefly discuss some aspects which are crucial for the further development of this approach towards the design of functional structures. Relying on a sequence of spontaneous assembly processes one necessarily goes down the free energy ladder and, therefore, the whole process is critically dependent on the energy landscape of the systems, i.e., the enthalpy difference between steps and the activation barriers associated with each processing step. For rather weakly interacting systems such as C_{60}, the available enthalpy range is small, thus, limiting the opportunities for a yield-optimised capturing of guest molecules. Minimisation of pore residues by tweaking the preparation conditions of the supramolecular network and the purity of chemicals are the options in this case but it is unclear whether, for the simple solution based processing applied here, the variations can be kept within the affordable tolerances. For this reason more strongly adsorbing systems like thiols appear better suited. However, exploiting kinetic control in such cases requires a careful design of the energy landscape and, clearly, in the present case the facile displacement of the star molecule is the bottleneck.

While increasing the stability of the pore modifier by a stronger bonding to the substrate seems an obvious solution to the problem, this raises the more fundamental questions to what extent an increased stability affects the dynamics and how the change in dynamics influences the assembly process. Since adsorption at the liquid solid interface is an exchange process between solvent molecules and the adsorbate, adsorption sites become available either by desorption of a solvent molecule of by surface diffusion. Therefore, the rate of exchange is expected to strongly depend on dimensions. In a highly confined space such as a single compartment of the star-network hybrid structure, lateral diffusion is impeded. If the lateral pathway becomes unavailable exchange can only occur via the third dimension, a process which is also strongly dependent on the sterical configuration. Thus it might well be that a too rigid compartment geometry defined by a strongly adsorbed pore modifier is not the optimal solution but a compromise between flexibility and stability being more advisable.

Experimental

Synthesis: The syntheses of **3BPEB-H** and **3BPEB-OH** have been described before.[47] Details for **4BPEB-2OH** are described in ESI.

Network preparation and adsorption of star molecules: Preparation of the PTCDI/melamine network was performed as described previously.[47, 68] In short, Au on mica substrates were flame-annealed in an oxygen rich natural gas flame before use and immersed in a PTCDI/melamine solution at 100 °C for 1 minute after which they were quickly rinsed with dimethyl formamide (DMF) at room temperature and immediately dried in a nitrogen stream.

The star molecules were adsorbed either from 1,2,4-trichlorobenzene (TCB) or DMF by immersion of the network modified substrate at 60°C. During the adsorption time of about two minutes the solution was cooling down. After removal from the solution, substrates were quickly blown dry in a stream of nitrogen. Due to the small amounts of substances available, the concentrations of the solutions of the star molecules were not exactly known and, therefore, immersion times were determined empirically by verifying that the adsorption times are sufficiently long for the formation of a full monolayer of star molecules on a clean Au substrate.

For the adsorption of C_{60} the sample was immersed in a TCB solution of the fullerene at 60°C with the solution cooling down during the exposure time of about 2 minutes. The adsorption of adamantane thiol was performed at the melting point of ethanol. For this a 10 μmolar solution of the thiol in ethanol was put in a vial and cooled down with liquid nitrogen. The sample was placed on the solidified mixture and when exposing the vial to room temperature the sample was immersed upon melting of the thiol/ethanol mixture. To keep the temperature at its minimum immersion was done while the thiol/ethanol mixture was in the two phase solid/liquid state.

Characterisation: Samples were imaged in an ambient environment using a PicoPlus STM (Molecular Imaging). Tips were cut from Pt/Ir wire (80:20, 0.25 mm diameter, Advent Research Materials Ltd.). Bias and current were typically in the range of ±100-500 mV and 10-100 pA.

Conclusions

The stepwise spontaneous assembly of a four component molecular system was investigated involving compartmentation of pores of a hydrogen bonded network as a key step followed by the templated adsorption of guest molecules into the subpores. The structural refinement of a porous network structure by nesting with another molecule introduces additional degrees of freedom in the ultraprecise design of surface based molecular structures. Furthermore it eliminates the uncertainties associated with the usual approach of network modification where the use of derivatised network components might result in a change of the network structure and/or polymorphism due to changes in interactions. The pore modifier adsorbing into the pores in high yield, the approach taken here should be rather straightforwardly extendable to different geometries and functionalisation of the pore modifier. The latter will also be important for controlling the dynamical behaviour of the oligo-(biphenyl-ethynyl)benzene molecules.

Concluding from the experiments that the dynamics of the pore modifier involves a partial intermittent detachment of the molecule, restricting mobility to the surface plane is considered crucial for the stability of the system and, thus, the control of adsorption of guest molecules. Showing that the templating of guest molecules by the pore modified network structure is feasible, a move towards functional structures will require improvement in the yield of the templated adsorption. Our experiments suggest that the level of perfection which can be achieved by adsorbing weakly interacting guest species under thermodynamically controlled conditions will be limited due to the imperfections in the synthesis of the network and the solution based processing. Kinetic control offering a solution to the problem, the adsorption strength of the pore modifier has to be improved in order to avoid its displacement by guest molecules which currently limits the adsorption conditions and the extent of guest templating.

Acknowledgements

This work was supported in part by The Leverhulme Trust (grant no. RPG-2013-177). The synthetic chemistry team thanks the Swiss National Science Foundation (SNF, grant no. 200020-159730) for continuous and generous financial support. We are grateful to A. Khlobystov for provision of the C_{60}. BK acknowledges EaStCHEM and the Funds for Women Graduates (FfWG) for postgraduate studentships.

Notes and references

1. C.-A. Palma, M. Cecchini and P. Samori, *Chem. Soc. Rev.*, 2012, **41**, 3713-3730.
2. N. Lin, S. Stepanow, F. Vidal, K. Kern, M. S. Alam, S. Stromsdorfer, V. Dremov, P. Muller, A. Landa and M. Ruben, *Dalton Transactions*, 2006, 2794-2800.
3. J. V. Barth, *Annu. Rev. Phys. Chem.*, 2007, **58**, 375-407.
4. A. Ciesielski, C.-A. Palma, M. Bonini and P. Samorì, *Adv. Mater.*, 2010, **22**, 3506-3520.
5. J. Teyssandier, S. D. Feyter and K. S. Mali, *Chem. Commun.*, 2016, **52**, 11465-11487.
6. S. Yoshimoto, Y. Honda, O. Ito and K. Itaya, *J. Am. Chem. Soc.*, 2008, **130**, 1085-1092.
7. H. Liang, Y. He, Y. C. Ye, X. G. Xu, F. Cheng, W. Sun, X. Shao, Y. F. Wang, J. L. Li and K. Wu, *Coord. Chem. Rev.*, 2009, **253**, 2959-2979.
8. N. A. Wasio, R. C. Quardokus, R. P. Forrest, C. S. Lent, S. A. Corcelli, J. A. Christie, K. W. Henderson and S. A. Kandel, *Nature*, 2014, **507**, 86-89.
9. L.-J. Wan, *Acc. Chem. Res.*, 2006, **39**, 334-342.
10. M. El Garah, A. Dianat, A. Cadeddu, R. Gutierrez, M. Cecchini, T. R. Cook, A. Ciesielski, P. J. Stang, G. Cuniberti and P. Samori, *Small*, 2016, **12**, 343-350.
11. S. Uemura, R. Tanoue, N. Yilmaz, A. Ohira and M. Kunitake, *Materials*, 2010, **3**, 4252-4276.
12. S.-L. Lee, Y. Fang, G. Velpula, F. P. Cometto, M. Lingenfelder, K. Müllen, K. S. Mali and S. De Feyter, *ACS Nano*, 2015, **9**, 11608-11617.
13. A. G. Slater, P. H. Beton and N. R. Champness, *Chem. Sci.*, 2011, **2**, 1440-1448.
14. J. Elemans, S. B. Lei and S. De Feyter, *Angew. Chem. Int. Ed.*, 2009, **48**, 7298-7332.
15. J. Lu, D.-L. Bao, H. Dong, K. Qian, S. Zhang, J. Liu, Y. Zhang, X. Lin, S.-X. Du, W. Hu and H.-J. Gao, *J. Phys, Chem. Lett.*, 2017, **8**, 326-331.
16. D. Nieckarz and P. Szabelski, *Chem. Commun.*, 2014, **50**, 6843-6845.
17. P. Szabelski, W. Rzysko, T. Panczyk, E. Ghijsens, K. Tahara, Y. Tobe and S. De Feyter, *RSC Advances*, 2013, **3**, 25159-25165.
18. T. Kudernac, S. B. Lei, J. Elemans and S. De Feyter, *Chem. Soc. Rev.*, 2009, **38**, 402-421.
19. X. Zhang, N. Li, L. Liu, G. Gu, C. Li, H. Tang, L. Peng, S. Hou and Y. Wang, *Chem. Commun.*, 2016, **52**, 10578-10581.
20. C.-A. Palma, A. Ciesielski, M. A. Oner, G. Schaeffer, J.-M. Lehn, J. V. Barth and P. Samori, *Chem. Commun.*, 2015, **51**, 17297-17300.
21. L. Piot, F. Silly, L. Tortech, Y. Nicolas, P. Blanchard, J. Roncali and D. Fichou, *J. Am. Chem. Soc.*, 2009, **131**, 12864-12865.
22. D. Grumelli, B. Wurster, S. Stepanow and K. Kern, *Nature Communications*, 2013, **4**, 2904.
23. D. den Boer, T. Habets, M. J. J. Coenen, M. van der Maas, T. P. J. Peters, M. J. Crossley, T. Khoury, A. E. Rowan, R. J. M. Nolte, S. Speller and J. A. A. W. Elemans, *Langmuir*, 2011, **27**, 2644-2651.
24. A. G. Slater, L. M. A. Perdigão, P. H. Beton and N. R. Champness, *Acc. Chem. Res.*, 2014, **47**, 3417-3427.
25. X. Bouju, C. Mattioli, G. Franc, A. Pujol and A. Gourdon, *Chem. Rev.*, 2017, **117**, 1407-1444.
26. R. Decker, U. Schlickum, F. Klappenberger, G. Zoppellaro, S. Klyatskaya, M. Ruben, J. V. Barth and H. Brune, *Appl. Phys. Lett.*, 2008, **93**, 243102.
27. S. Stepanow, N. Lin, J. V. Barth and K. Kern, *Chem. Commun.*, 2006, 2153-2155.
28. S. Stepanow, M. Lingenfelder, A. Dmitriev, H. Spillmann, E. Delvigne, N. Lin, X. B. Deng, C. Z. Cai, J. V. Barth and K. Kern, *Nature Mat.*, 2004, **3**, 229-233.
29. S. Fabris, S. Stepanow, N. Lin, P. Gambardella, A. Dmitriev, J. Honolka, S. Baroni and K. Kern, *Nano Lett.*, 2011, **11**, 5414-5420.
30. W. Xiao, D. Passerone, P. Ruffieux, K. Aït−Mansour, O. Gröning, E. Tosatti, J. S. Siegel and R. Fasel, *J. Am. Chem. Soc.*, 2008, **130**, 4767-4771.

31. D. Bonifazi, A. Kiebele, M. Stöhr, F. Cheng, T. Jung, F. Diederich and H. Spillmann, *Adv. Funct. Mater.*, 2007, **17**, 1051-1062.
32. A. G. Phillips, L. M. A. Perdigao, P. H. Beton and N. R. Champness, *Chem. Commun.*, 2010, **46**, 2775-2777.
33. S. J. H. Griessl, M. Lackinger, F. Jamitzky, T. Markert, M. Hietschold and W. M. Heckl, *J. Phys. Chem. B*, 2004, **108**, 11556-11560.
34. J. A. Theobald, N. S. Oxtoby, M. A. Phillips, N. R. Champness and P. H. Beton, *Nature*, 2003, **424**, 1029-1031.
35. E. Mena-Osteritz and P. Bauerle, *Adv. Mater.*, 2006, **18**, 447-451.
36. K. H. Chung, H. Kim, W. J. Jang, J. K. Yoon, S. J. Kahng, J. Lee and S. Han, *J. Phys. Chem. C*, 2013, **117**, 302-306.
37. J. Teyssandier, S. De Feyter and K. S. Mali, *Chem. Commun.*, 2016, **52**, 11465-11487.
38. S. Klyatskaya, F. Klappenberger, U. Schlickum, D. Kuhne, M. Marschall, J. Reichert, R. Decker, W. Krenner, G. Zoppellaro, H. Brune, J. V. Barth and M. Ruben, *Adv. Funct. Mater.*, 2011, **21**, 1230-1240.
39. K. Cui, F. Schluetter, O. Ivasenko, M. Kivala, M. G. Schwab, S.-L. Lee, S. F. L. Mertens, K. Tahara, Y. Tobe, K. Muellen, K. S. Mali and S. De Feyter, *Chem. Eur. J.*, 2015, **21**, 1652-1659.
40. S. Q. Zhang, J. Y. Zhang, K. Deng, J. L. Xie, W. B. Duan and Q. D. Zeng, *Phys. Chem. Chem. Phys.*, 2015, **17**, 24462-24467.
41. J. Adisoejoso, K. Tahara, S. Okuhata, S. Lei, Y. Tobe and S. De Feyter, *Angew. Chem. Int. Ed.*, 2009, **48**, 7353-7357.
42. R. Madueno, M. T. Raisanen, C. Silien and M. Buck, *Nature*, 2008, **454**, 618-621.
43. C. Silien, M. T. Räisänen and M. Buck, *Angew. Chem. Int. Ed.*, 2009, **48**, 3349-3352.
44. C. Silien, M. T. Räisänen and M. Buck, *Small*, 2010, **6**, 391-394.
45. M. T. Räisänen, A. G. Slater, N. R. Champness and M. Buck, *Chem. Sci.*, 2012, **3**, 84-92.
46. L. M. A. Perdigao, A. Saywell, G. N. Fontes, P. A. Staniec, G. Goretzki, A. G. Phillips, N. R. Champness and P. H. Beton, *Chem. Eur. J.*, 2008, **14**, 7600-7607.
47. B. Karamzadeh, T. Eaton, I. Cebula, D. M. Torres, M. Neuburger, M. Mayor and M. Buck, *Chem. Commun.*, 2014, **50**, 14175-14178.
48. D. Bléger, D. Kreher, F. Mathevet, A.-J. Attias, G. Schull, A. Huard, L. Douillard, C. Fiorini-Debuischert and F. Charra, *Angew. Chem. Int. Ed.*, 2007, **46**, 7404-7407.
49. G.-B. Pan, J.-M. Liu, H.-M. Zhang, L.-J. Wan, Q.-Y. Zheng and C.-L. Bai, *Angew. Chem. Int. Ed.*, 2003, **42**, 2747-2751.
50. M. Li, K. Deng, S.-B. Lei, Y.-L. Yang, T.-S. Wang, Y.-T. Shen, C.-R. Wang, Q.-D. Zeng and C. Wang, *Angew. Chem. Int. Ed.*, 2008, **47**, 6717-6721.
51. H. Spillmann, A. Kiebele, M. Stohr, T. A. Jung, D. Bonifazi, F. Y. Cheng and F. Diederich, *Adv. Mater.*, 2006, **18**, 275-279.
52. L. M. A. Perdigao, P. A. Staniec, N. R. Champness and P. H. Beton, *Langmuir*, 2009, **25**, 2278-2281.
53. N. M. Jenny, M. Mayor and T. R. Eaton, *Eur. J. Org. Chem.*, 2011, 4965-4983.
54. E. A. Krasnokutskaya, N. I. Semenischeva, V. D. Filimonov and P. Knochel, *Synthesis*, 2007, 81-84.
55. T. Waldmann, R. Reichert and H. E. Hoster, *ChemPhysChem*, 2010, **11**, 1513-1517.
56. T. Waldmann, J. Klein, H. E. Hoster and R. J. Behm, *ChemPhysChem*, 2013, **14**, 162-169.
57. N. Wintjes, D. Bonifazi, F. Y. Cheng, A. Kiebele, M. Stohr, T. Jung, H. Spillmann and F. Diederich, *Angew. Chem. Int. Ed.*, 2007, **46**, 4089-4092.
58. A. E. Baber, H. L. Tierney and E. C. H. Sykes, *ACS Nano*, 2008, **2**, 2385-2391.
59. D. Kühne, F. Klappenberger, W. Krenner, S. Klyatskaya, M. Ruben and J. V. Barth, *Proc. Natl. Acad. Sci.*, 2010, **107**, 21332–21336.
60. J. K. Gimzewski, C. Joachim, R. R. Schlittler, V. Langlais, H. Tang and I. Johannsen, *Science*, 1998, **281**, 531-533.
61. S. J. H. Griessl, M. Lackinger, F. Jamitzky, T. Markert, M. Hietschold and W. A. Heckl, *Langmuir*, 2004, **20**, 9403-9407.
62. B. Karamzadeh, T. Eaton, I. Cebula, D. M. Torres, M. Neuburger, M. Mayor and M. Buck, CCDC 1000630 (2014) DOI: 10.5517/cc12l7d9.
63. D. Écija, K. Seufert, D. Heim, W. Auwärter, C. Aurisicchio, C. Fabbro, D. Bonifazi and J. V. Barth, *ACS Nano*, 2010, **4**, 4936-4942.
64. D. Heim, D. Écija, K. Seufert, W. Auwärter, C. Aurisicchio, C. Fabbro, D. Bonifazi and J. V. Barth, *J. Am. Chem. Soc.*, 2010, **132**, 6783-6790.
65. T. Takeda and Y. Tobe, *Chem. Commun.*, 2012, **48**, 7841-7843.
66. G. Jeschke, M. Sajid, M. Schulte, N. Ramezanian, A. Volkov, H. Zimmermann and A. Godt, *J. Am. Chem. Soc.*, 2010, **132**, 10107-10117.
67. C. A. Palma, J. Bjork, F. Rao, D. Kuhne, F. Klappenberger and J. V. Barth, *Nano Lett.*, 2014, **14**, 4461-4468.
68. I. Cebula, M. T. Raisanen, R. Madueno, B. Karamzadeh and M. Buck, *Phys. Chem. Chem. Phys.*, 2013, **15**, 14126.